Priority Issue 9
to be Tackled by Using Post K Computer
"Elucidation of the Fundamental Laws
and Evolution of the Universe"
KAKENHI grant 17K05433, 25870168

CNS Summer school 2019
2019/08/21-27, Hongo, The University of Tokyo

Nuclear shell model calculations – basics and practices –

3. Inside "KSHELL"

Noritaka Shimizu

Center for Nuclear Study,
the University of Tokyo

Hamiltonian matrix in the LSSM

⇒ Real symmetric sparse matrix

Nuclide	Space	Basis dim.	Sparsity	Storage (GB)
^{28}Si	sd	9.4×10^4	6×10^{-3}	0.2
^{52}Fe	pf	1.1×10^8	1×10^{-5}	720
^{56}Ni	pf	1.1×10^9	2×10^{-6}	9600

^{44}Ti M=0 space in pf-shell (4,000 dim.)

C.W. Johnson *et al*., CPC 2013

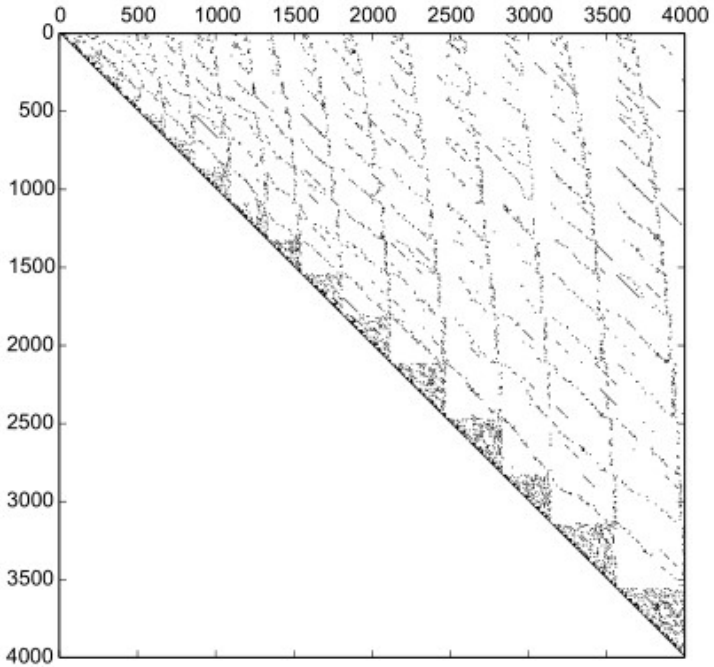

- The Lanczos algorithm is quite efficient to obtain low-lying states.
- In the KSHELL code, the matrix elements of the many-body Hamiltonian is generated on-the-fly every matrix-vector product to suppress the memory usage.

Truncation of the model space

^{56}Ni ... Z=N=28 doubly closed with N=Z=28 magic, truncation of particle-hole excitation is expected to work well

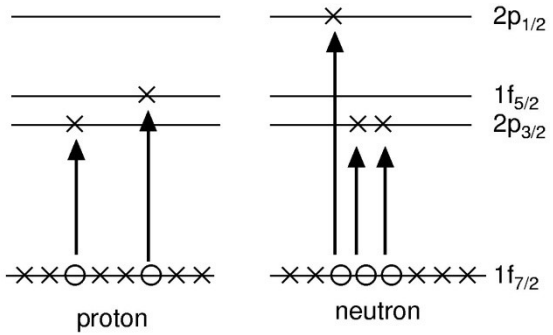

Number of p-h excitation from f7/2 is restricted (*t*)

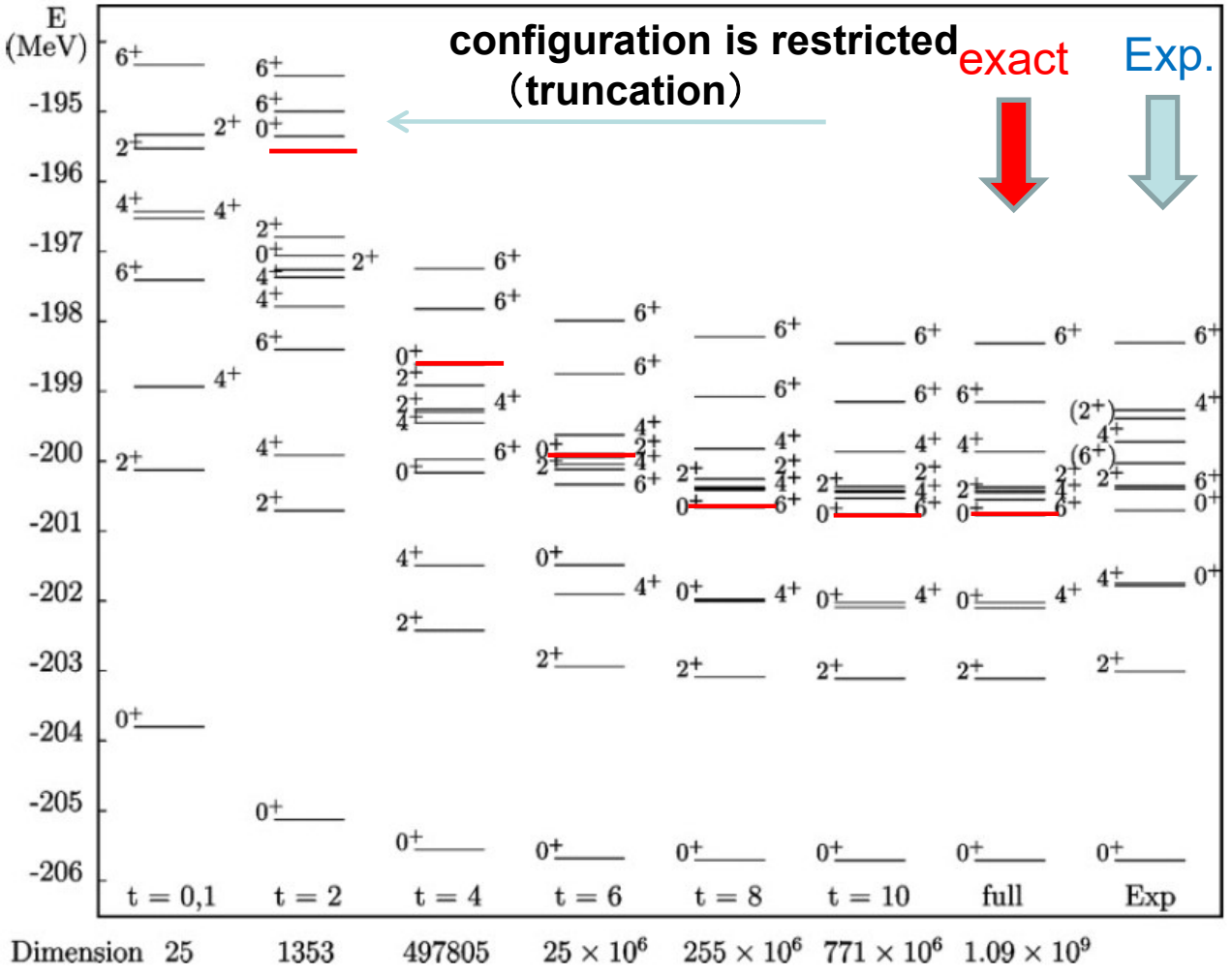

Ref. M. Horoi *et al.*, Phys. Rev. C78, 014318(2008)

Truncation by $N\hbar\omega$ excitation

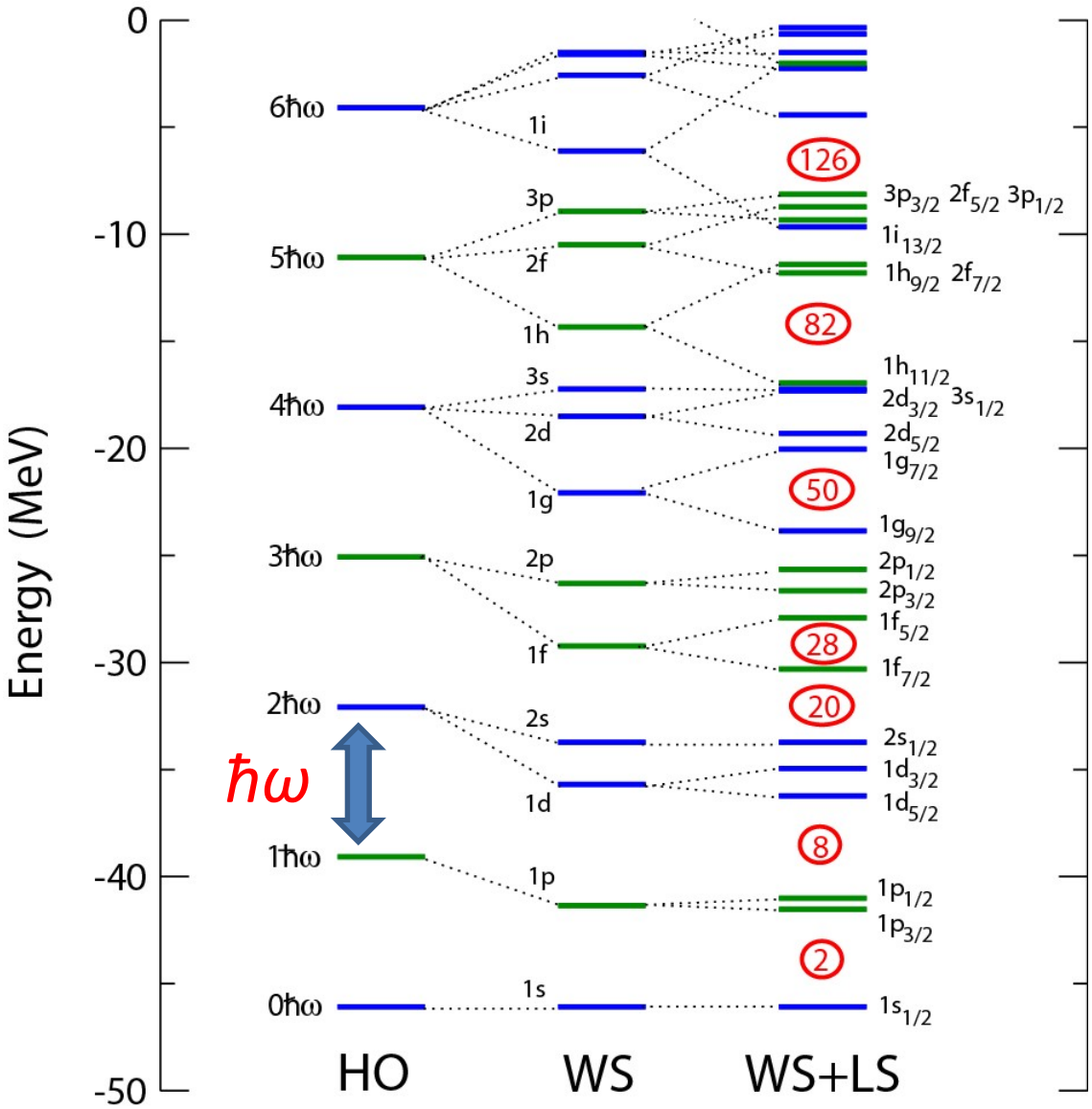

$0\hbar\omega$

no cross shell excitation

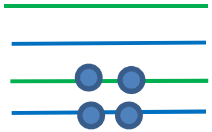

$2\hbar\omega$

across 2 shell gaps

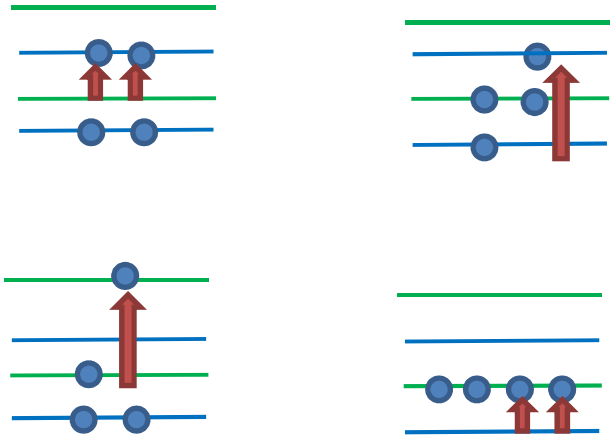

and so on ...

Contamination of center-of-mass motion

- In the model space beyond 0$\hbar\omega$, center-of-mass motion is contaminated.
- Lawson method
  - Lift up spurious center-of-mass excited states by adding CoM Hamiltonian

$$H' = H + \beta_{\mathrm{CM}} H_{\mathrm{CM}}$$

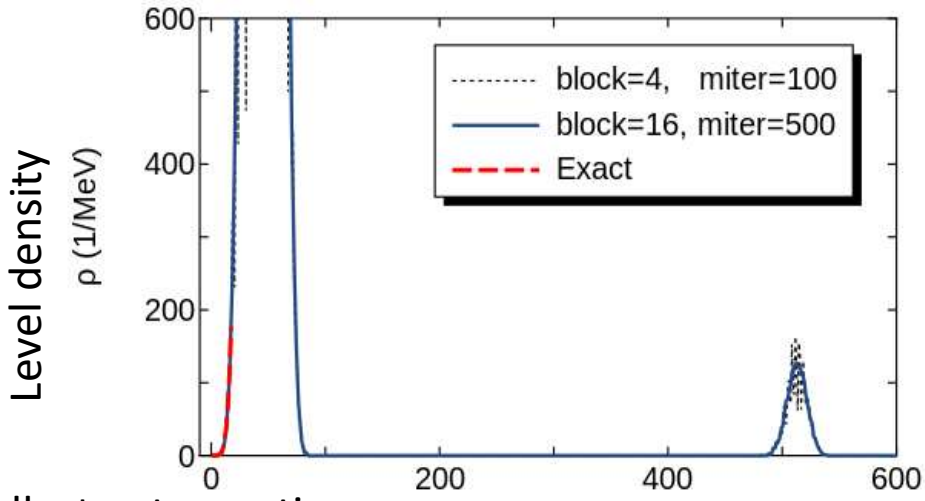

^{48}Ca J=1^{-}, sd-pf-sdg shell, 1ħω truncation

- Center-of-mass motion can be clearly removed in full $N\hbar\omega$ model space
- If not full space, separation is approximately achieved by large β_{CM} … controversial

Truncation in KSHELL code

```
truncation scheme ?
      0 : No truncation (default)
      1 : particle-hole truncation for orbit(s)
      2 : hw truncation
      3 : Both (1) and (2)

1
   #    n,  l,  j, tz,    spe
   1    0   3   7  -1    -8.624     p_0f7/2
   2    1   1   3  -1    -5.679     p_1p3/2
   3    0   3   5  -1    -1.383     p_0f5/2
   4    1   1   1  -1    -4.137     p_1p1/2
   5    0   3   7   1    -8.624     n_0f7/2
   6    1   1   3   1    -5.679     n_1p3/2
   7    0   3   5   1    -1.383     n_0f5/2
   8    1   1   1   1    -4.137     n_1p1/2
 specify # of orbit(s) and min., max. occupation numbers for restriction

 # of orbit(s) for restriction?  (<CR> to quit): 2,3,4,6,7,8
 min., max. restricted occupation numbersfor the orbit(s) (or max only) : 0,2

 # of orbit(s) for restriction?  (<CR> to quit):
```

Advanced option: one-body transition density

- Concerning the transition and moments, it would be better to replace the H.O. wave function by e.g. Woods-Saxon wave function.
- In this case, the KSHELL code provides one-body transition density (OBTD) by “is_obtd=.true.” option.

$$< f||\hat{O}^{\lambda}||i > =< n\omega J||\hat{O}^{\lambda}||n\omega' J' >= \sum_{k_\alpha k_\beta} \mathrm{OBTD}(fik_\alpha k_\beta \lambda) < k_\alpha||O^{\lambda}||k_\beta >$$

$$\mathrm{OBTD}(fik_\alpha k_\beta \lambda) = \frac{< n\omega J||[a^{+}_{k_\alpha} \otimes \tilde{a}_{k_\beta}]^{\lambda}||n\omega' J' >}{\sqrt{(2\lambda+1)}}$$

Pitfall : Phase convention

For further study, you may want to construct your own operator. Pay attention to phase conventions.

- Condon-Shortley vs. Biedenharn-Rose convention
  - $Y_m^{(l)}(\theta,\phi) \quad \Leftrightarrow \quad i^l Y_m^{(l)}(\theta,\phi)$
- spin-orbit coupling
  - $j = l + s \quad \Leftrightarrow \quad j = s + l$
- Radial wave function
  - $R_{nl}(+\varepsilon) > 0 \Leftrightarrow R_{nl}(+\infty) > 0$
  - $n = 0,1,2,\ldots \Leftrightarrow n = 1,2,3,\ldots$

Lanczos method

- Suppose large real symmetric sparse matrix and obtain some lowest eigenvalues...
- One of the Krylov-subspace methods

$$\mathcal{K}_{l_m}(H, \boldsymbol{v}_1) = \{\boldsymbol{v}_1, H\boldsymbol{v}_1, H^2\boldsymbol{v}_1, H^3\boldsymbol{v}_1, \cdots, H^{l_m-1}\boldsymbol{v}_1\}$$

- Ritz value ... eigenvalues of submatrix in Krylov subspace

Power method

- Suppose large real symmetric sparse matrix and obtain the lowest (largest) eigenvalues...

$$x_0 = e_n v_n + e_{n-1} v_{n-1} \ldots + e_1 v_1$$

$$x_k = H^k x_0$$

$$= (e_n)^k v_n + (e_{n-1})^k v_{n-1} \ldots + (e_1)^k v_1$$

$$\rightarrow v_1$$ Converges to largest absolute eigenvalue

$$\frac{x_k^T H x_{k-1}}{x_{k-1}^T x_{k-1}} \rightarrow e_1$$

Lanczos method : algorithm

- Prepare initial state (e.g. random) u_0
- Iterate

Matrix-vector product, bottle neck!

$$a_k = u_k^T A u_k \qquad b_k = u_k^T A u_{k-1}$$

Gram-Schmidt orthogonalization

$$u'_{k+1} = Au_k - a_k u_k - b_k u_{k-1}$$

Normalize

$$u_{k+1} = u'_{k+1} / \sqrt{u'^T_{k+1} u_{k+1}}$$

$$T = u_i^T A u_j = \begin{bmatrix} a_0 & b_0 & & & & \\ b_0 & a_1 & b_1 & & & \\ & b_1 & a_2 & b_3 & & \\ & & b_2 & a_3 & b_3 & \\ & & & b_3 & \dots & \dots \\ & & & & \dots & \dots \end{bmatrix}$$

- Solve eigenvalue problem of tri-diagonal matrix by bisection method

N.B. $u_i^T u_{k-1} = \delta_{ij}$ is satisfied mathematically. However, as k increases, this orthogonality relation is often broken by round-off error

→ Reorthonalization

Convergence of Lanczos method

^{56}Ni shell-model calc. 10^9-dimension sparse matrix ⟹ 4GB Lanczos vector

10 lowest eigenvalues ... 241 iterations

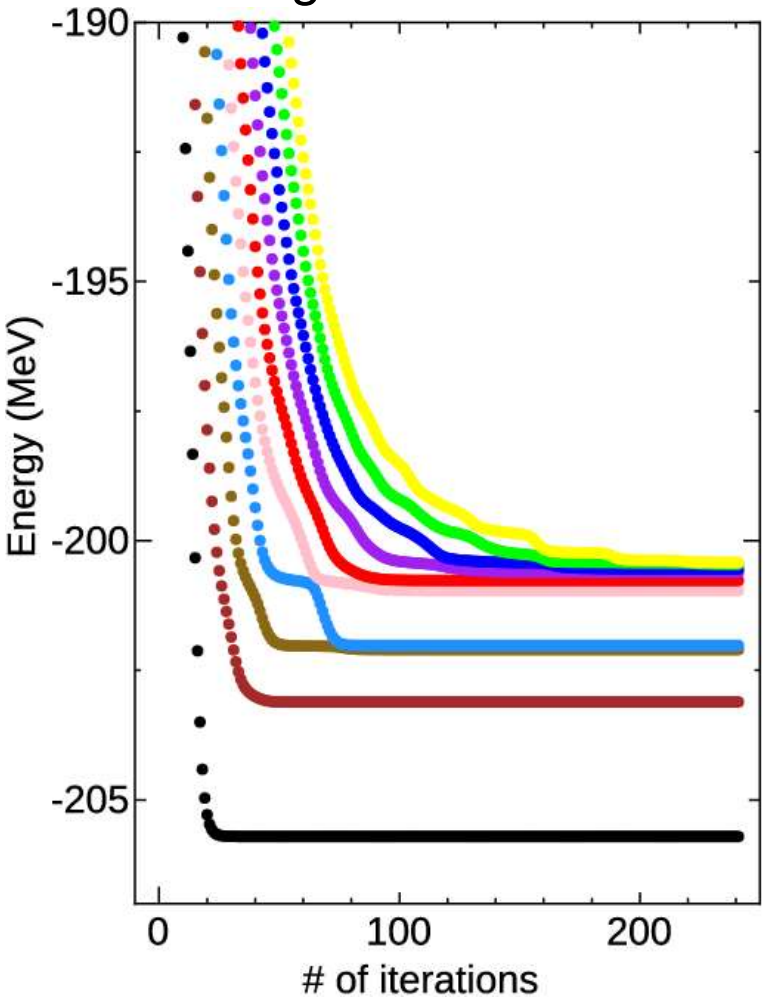

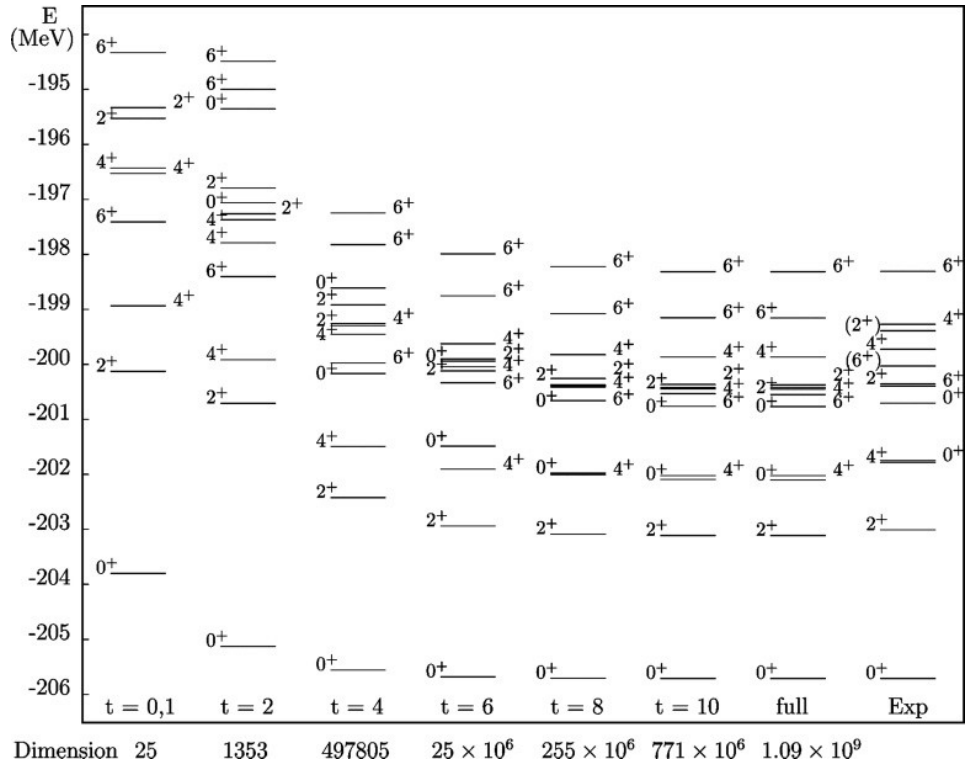

Excitation energies of ^{56}Ni

Ref. M. Horoi et al. Phys. Rev. C73 061305R (2006)

code “KSHELL”

9 sec/iteration @FX10 240 nodes (SPARC 64 IXfx, 3840 cores), total 35min.

Matrix representation

$$|\Psi\rangle = u_1$$ 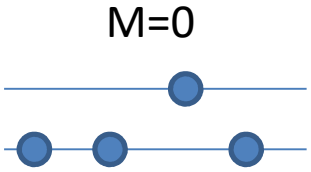

$$+ u_2$$ 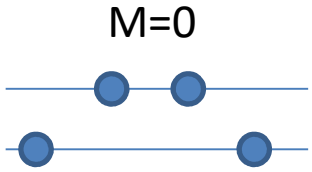

$$+ u_3$$ 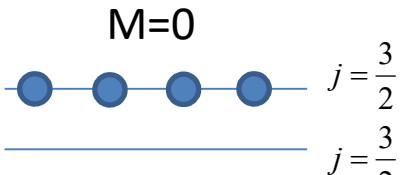

$$+\cdots$$

$$= u_1|m_1\rangle + u_2|m_2\rangle + u_3|m_3\rangle + \cdots$$

Solve eigenvalue problem of the Hamiltonian matrix

$$H_{ij} = \langle m_i | H | m_j \rangle$$

Why is it sparse matrix?

Hamiltonian is two-body (or three-body) interaction:

$$H = \sum_{ij} t_{ij} c_i^\dagger c_j + \sum_{ijkl} v_{ijkl} c_i^\dagger c_j^\dagger c_l c_k$$

e.g. $\langle m_1 | H | m_3 \rangle = 0$ for two-body int.

Configuration : bit representation

$$|\Psi\rangle = u_1$$ 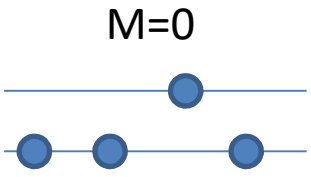

$$+ u_2$$ 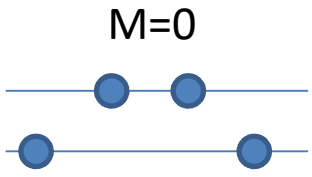

$$+ u_3$$ 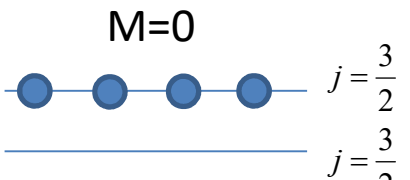

$$+\cdots$$

$$= u_1|m_1\rangle + u_2|m_2\rangle + u_3|m_3\rangle + \cdots$$

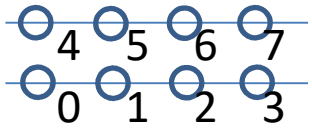

$$|m_1\rangle = c_0^\dagger c_1^\dagger c_3^\dagger c_6^\dagger |-\rangle$$

m	0	1	2	3	4	5	6	7	Decimal num.
$\|m_1\rangle$	1	1	0	1	0	0	1	0	75
$\|m_2\rangle$	1	0	0	1	0	1	1	0	105
$\|m_3\rangle$	0	0	0	0	1	1	1	1	240

“On-the-fly” operation of matrix-vector product

Number of Hamiltonian matrix element $H_{ij} = \langle m_i | H | m_j \rangle$ is too huge to store on memory

Only matrix-vector product is required for Lanczos method

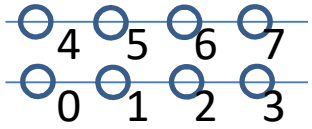

$$|m_3\rangle = c_4^\dagger c_7^\dagger c_1 c_0 |m_1\rangle$$

m	0	1	2	3	4	5	6	7	Decimal num.
$\|m_1\rangle$	1	1	0	1	0	0	1	0	75
$\|m_2\rangle$	1	0	0	1	0	1	1	0	105
$\|m_3\rangle$	0	0	0	0	1	1	1	1	240

$c_4^\dagger c_7^\dagger c_1 c_0$

off 1, 0 bits
and
on 4, 7 bits

Binary search to find where the obtained number is.

Further acceleration : proton-neutron factorization of wave function

Each *M*-scheme basis state is a product of proton and neutron configurations

$$\left|m\right\rangle = \left|m_\pi\right\rangle \otimes \left|m_\upsilon\right\rangle$$

$$M = M_p + M_n \qquad Jz$$

$$\Pi = \Pi_p \times \Pi_n \qquad \text{Parity}$$

$$\left|\Psi\right\rangle = \sum_m v_m \left|m\right\rangle = \sum_{M_p,\Pi_p} \sum_{\substack{m_p \in M_p,\Pi_p \\ m_n \in M_n,\Pi_n}} v_{m_\pi,m_\upsilon} \left|m_p\right\rangle \otimes \left|m_n\right\rangle$$

For acceleration of the matrix-vector product of the proton-neutron interaction（bottle neck）

$$c_i^\dagger c_j^\dagger c_l c_k \left| m_p^{(\pi)} \right\rangle \left| m_n^{(\nu)} \right\rangle = c_i^\dagger c_k \left| m_p^{(\pi)} \right\rangle c_j^\dagger c_l \left| m_n^{(\nu)} \right\rangle = \left| m_{p'}^{(\pi)} \right\rangle \left| m_{n'}^{(\nu)} \right\rangle$$

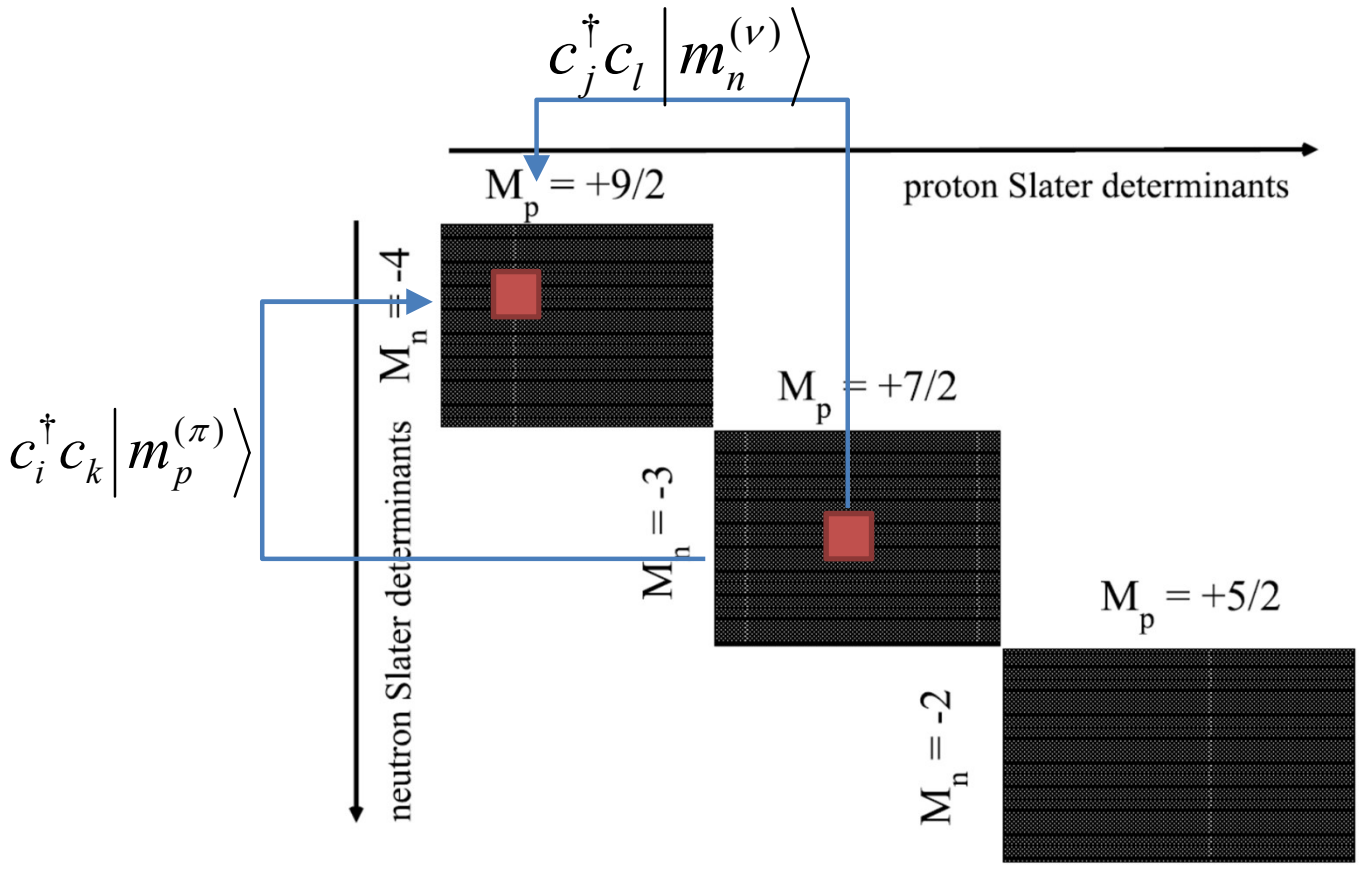

In advance, proton one-body interaction $c_i^\dagger c_k \left| m_p^{(\pi)} \right\rangle$ and neutron one-body interaction $c_j^\dagger c_l \left| m_n^{(\nu)} \right\rangle$ are operated to accelerate the proton-neutron interaction.

Block Lanczos method

- Block Krylov subspace method

$$\mathcal{K}_m(H, \boldsymbol{V}_1) = \{\boldsymbol{V}_1, H\boldsymbol{V}_1, H^2\boldsymbol{V}_1, \cdots, H^{m-1}\boldsymbol{V}_1\} \qquad \boldsymbol{V}_1 = \left(\boldsymbol{v}_1^{(1)}, \boldsymbol{v}_1^{(2)}, \cdots, \boldsymbol{v}_1^{(q)}\right)$$

a block of vectors $\boldsymbol{V}_1$ be arbitrary vectors with $\boldsymbol{V}_1^T\boldsymbol{V}_1 = \boldsymbol{1}$
and $\boldsymbol{\beta}_{-1} := \boldsymbol{0}$.
for $k = 1, 2, 3, \cdots$ **do**
  $\boldsymbol{W} := H\boldsymbol{V}_k$
  $\boldsymbol{\alpha}_k := \boldsymbol{V}_k^T\boldsymbol{W}$
  $T_{k(p-1)+1:kp,k(p-1)+1:kp} := \boldsymbol{\alpha}_k$
  Diagonalize $T^{(k)}$ and stop if e_n converges
  $\boldsymbol{W} = \boldsymbol{W} - \boldsymbol{V}_k\boldsymbol{\alpha}_k$
  Reorthogonalize $\boldsymbol{W}$ with $\{\boldsymbol{V}_1, \boldsymbol{V}_2, \cdots, \boldsymbol{V}_{k-1}\}$
  $\boldsymbol{V}_{k+1}\boldsymbol{\beta}_k = \mathrm{QR}(\boldsymbol{W})$
  $T_{k(p+1)+1:k(p+2),kp+1:k(p+1)} := \boldsymbol{\beta}_k$
  $T_{kp+1:k(p+1),k(p+1)+1:k(p+2)} := \boldsymbol{\beta}_k^T$,
end for

Subspace extended by a product of a matrix and block vectors

$$T^{(k)} = \begin{pmatrix} \boldsymbol{\alpha}_1 & \boldsymbol{\beta}_1^T & & & 0 \\ \boldsymbol{\beta}_1 & \boldsymbol{\alpha}_2 & \boldsymbol{\beta}_2^T & & \\ & \boldsymbol{\beta}_2 & \boldsymbol{\alpha}_3 & \ddots & \\ & & \ddots & \ddots & \boldsymbol{\beta}_{k-1}^T \\ 0 & & & \boldsymbol{\beta}_{k-1} & \boldsymbol{\alpha}_k \end{pmatrix}$$

$\boldsymbol{\alpha}_i$ and $\boldsymbol{\beta}_i$ are $p \times p$ block matrices

Performance improvement of block algorithm

Elapsed time of a product of the matrix and block vectors

$$(v'_1, v'_2, \ldots v'_p) = H(v_1, v_2, \ldots v_p)$$

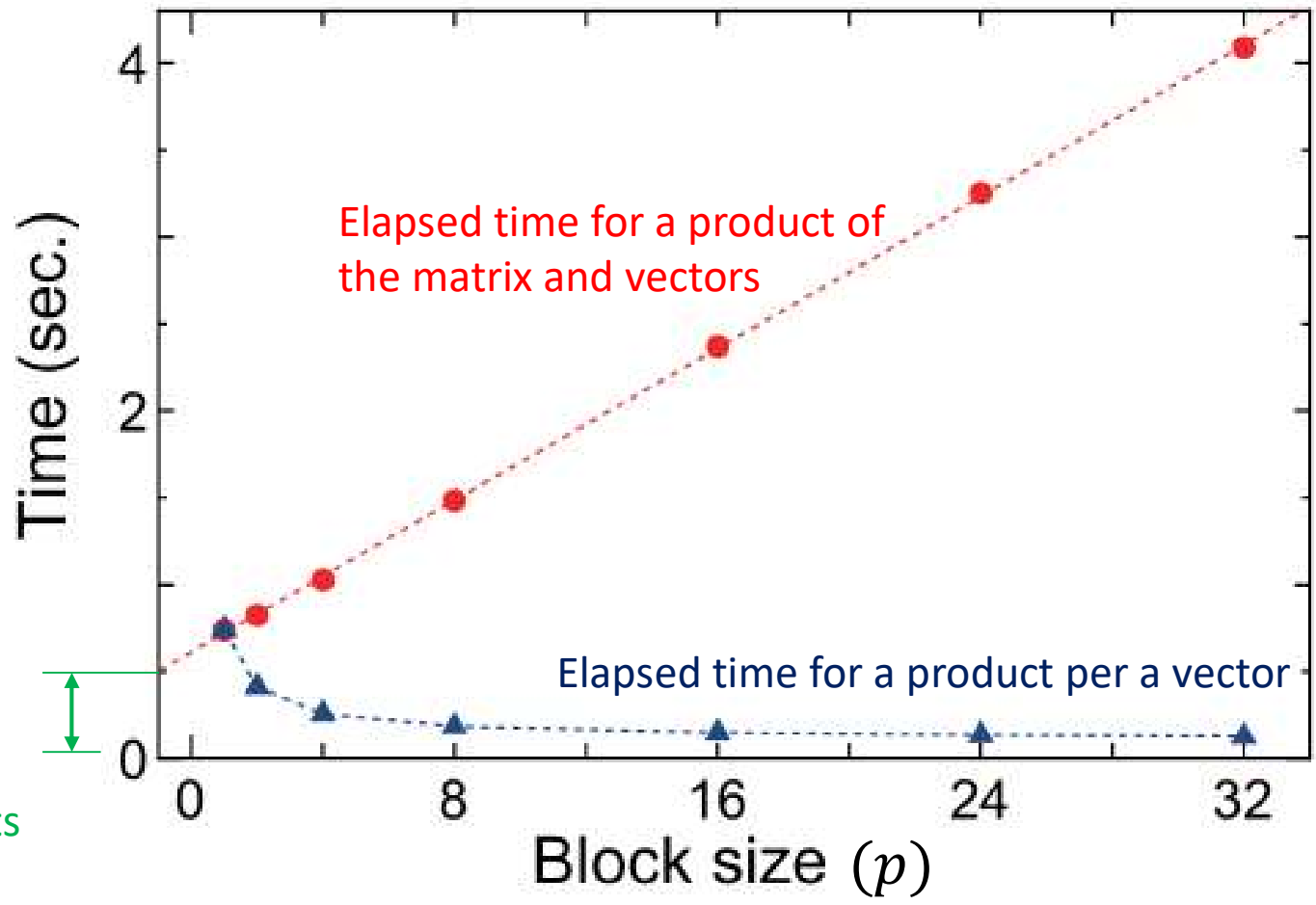

^{48}Cr in pf-shell, 1,963,461 dimension, Xeon 20 cores

Performance improvement by the block Lanczos method

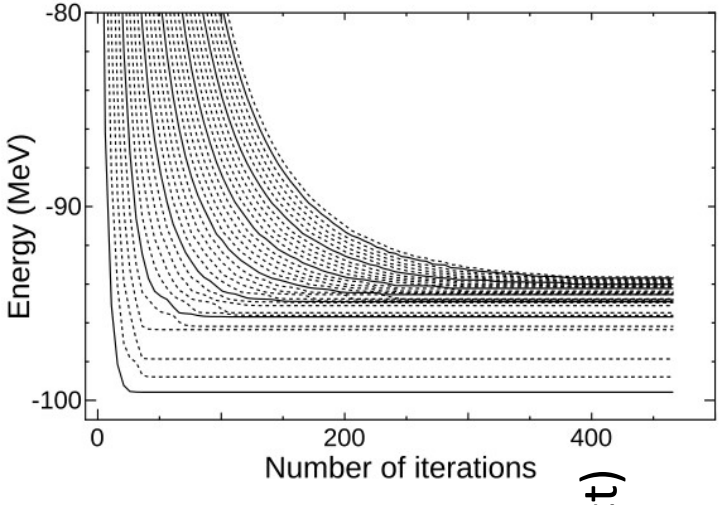

^{48}Cr in pf-shell, 1,963,461 dimension

Convergence of the 32nd eigenvalue

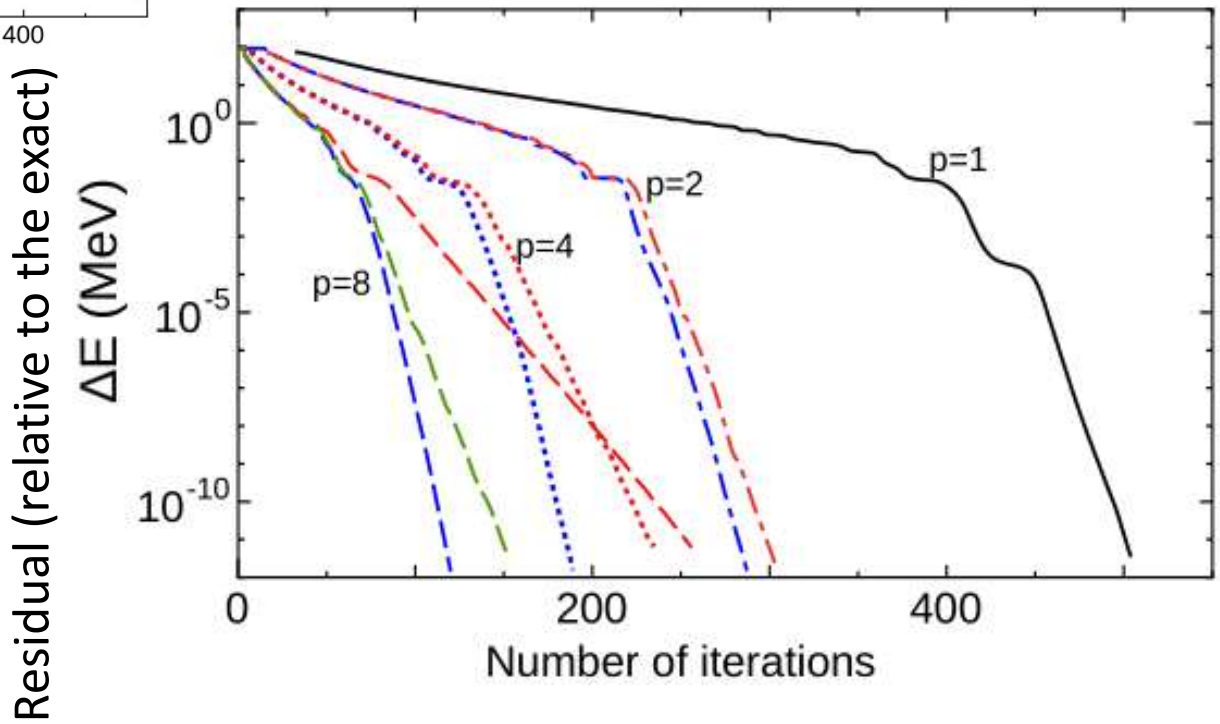

Performance of block Lanczos method

^{48}Cr in pf-shell, 1,963,461 dimension

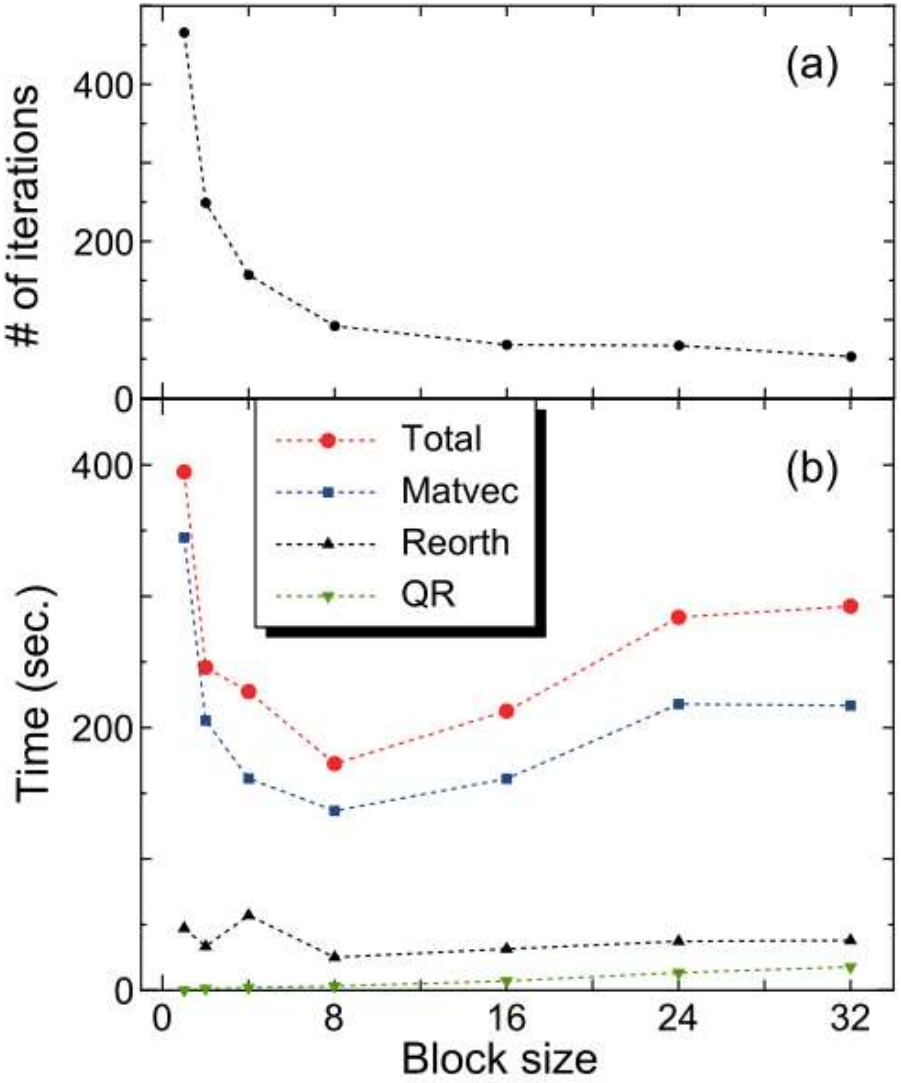

^{112}Sn w/ ^{100}Sn core

6,210,638 dimension

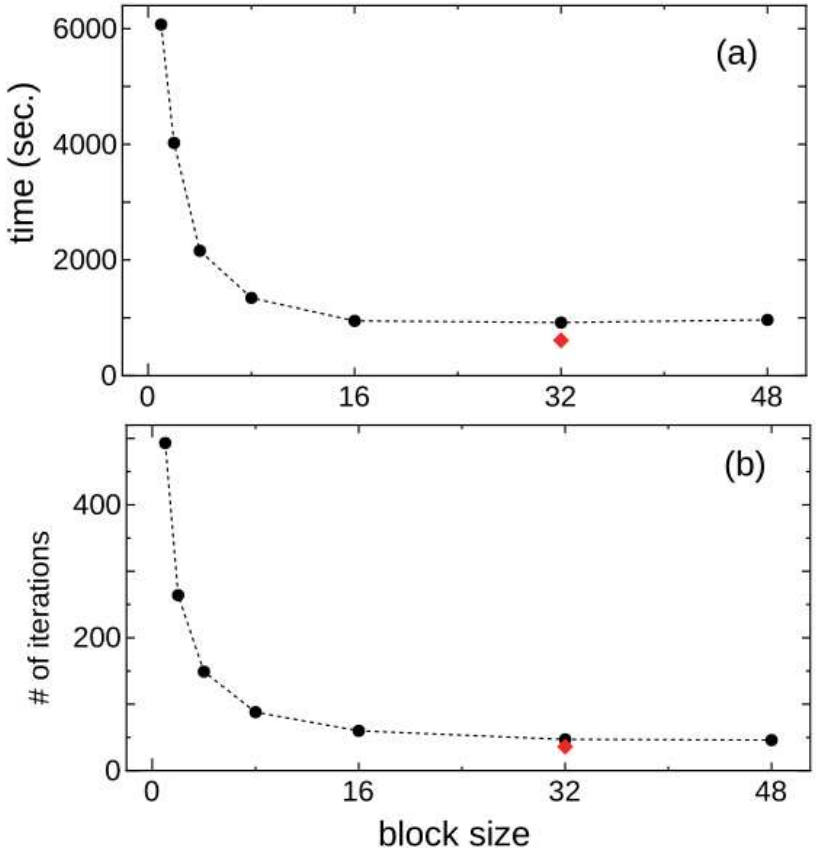

Further acceleration : Thick-restart block method

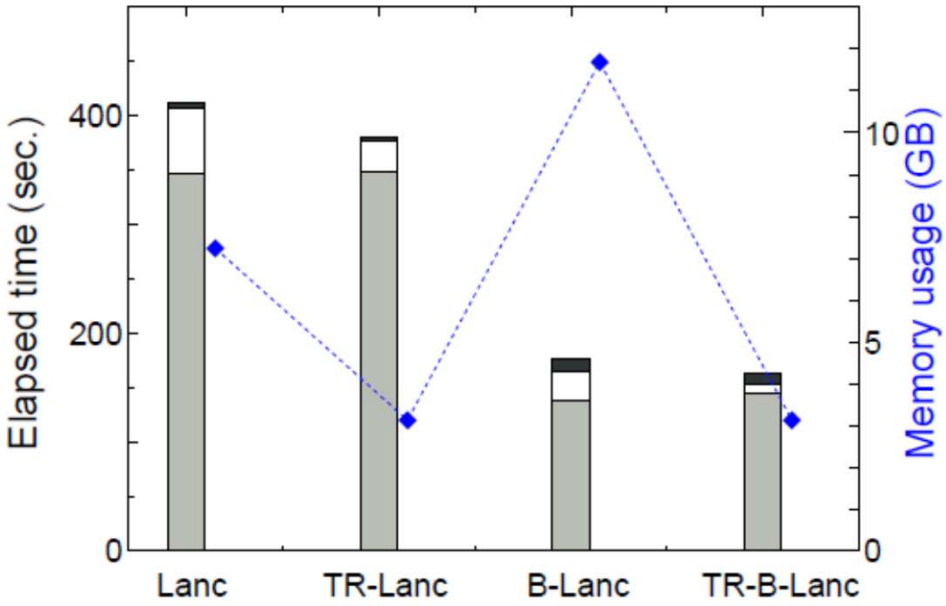

FIG. 8: Total elapsed time to obtain the 32 lowest eigenvalues of ^{48}Cr with the simple Lanczos (Lanc), thick-restart Lanczos (TR-Lanc), block Lanczos (B-Lanc), and thick-restart block Lanczos (TR-B-Lanc) methods. The shaded, open, and filled bars denote the elapsed times of matrix-vectors products, re-orthogonalizations, and the others, respectively. The memory usage to store the Lanczos vectors is shown as the blue diamonds with the dashed line. We take the block size $q = 8$ for the block methods and the maximum number of the Lanczos vectors $l_m = 200$ for the thick-restart methods.

When the number of the Lanczos vectors reaches $l_m = 200$, the 20 lowest eigenvectors in the subspace is only taken and restart the Lanczos iterations.

N. Shimizu et al., Comp. Phys. Comm. in print.

Massively parallel computation

Summit @ ORNL
17,579,520 GPU cores

K computer
548,352 CPU cores

2020 Japan will launch
“Fugaku” supercomputer

Parallel computation of matrix-vector product in the KSHELL code

E.g. assume 9 computer nodes

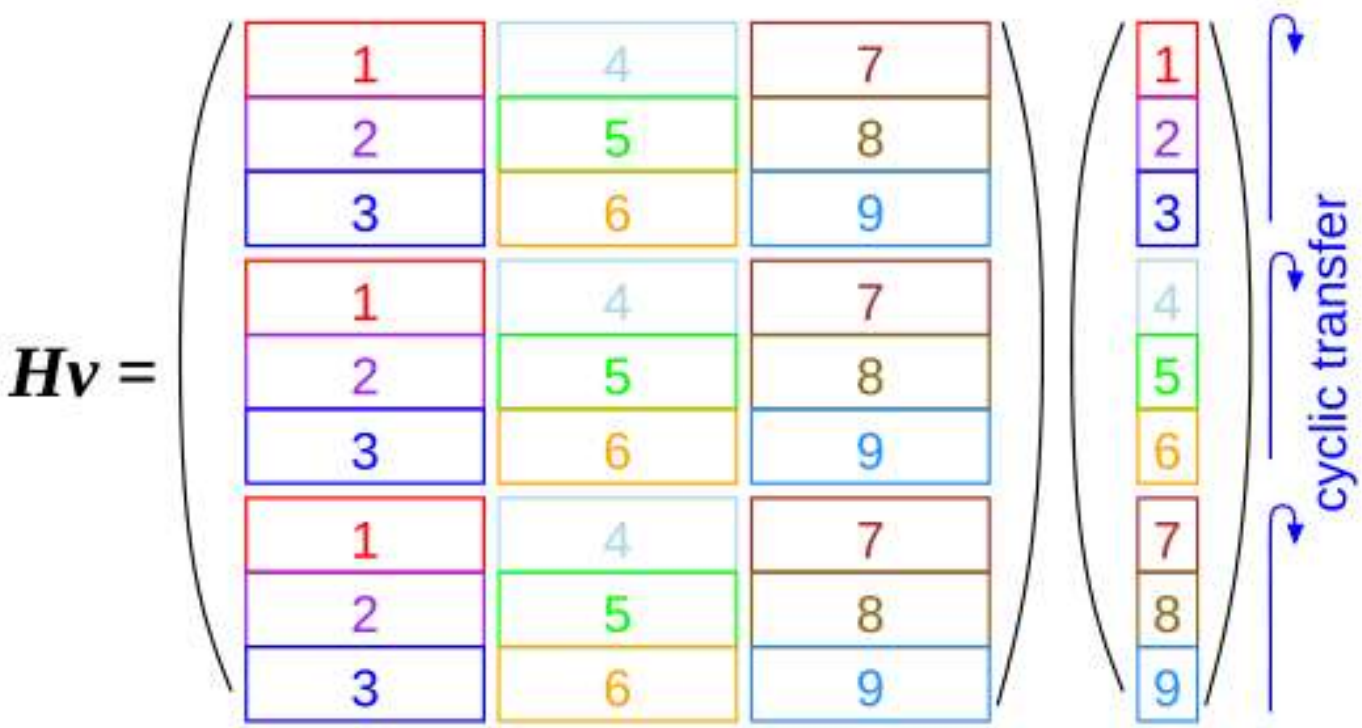

- Diagonal blocks are equally distributed.
- Communication volume per matrix-vector product is the smallest, $2V/\sqrt{N}$ (V: size of a vector, N: number of nodes)
- A vector is split equally for reorthogonalization

Parallel performance (strong scaling)

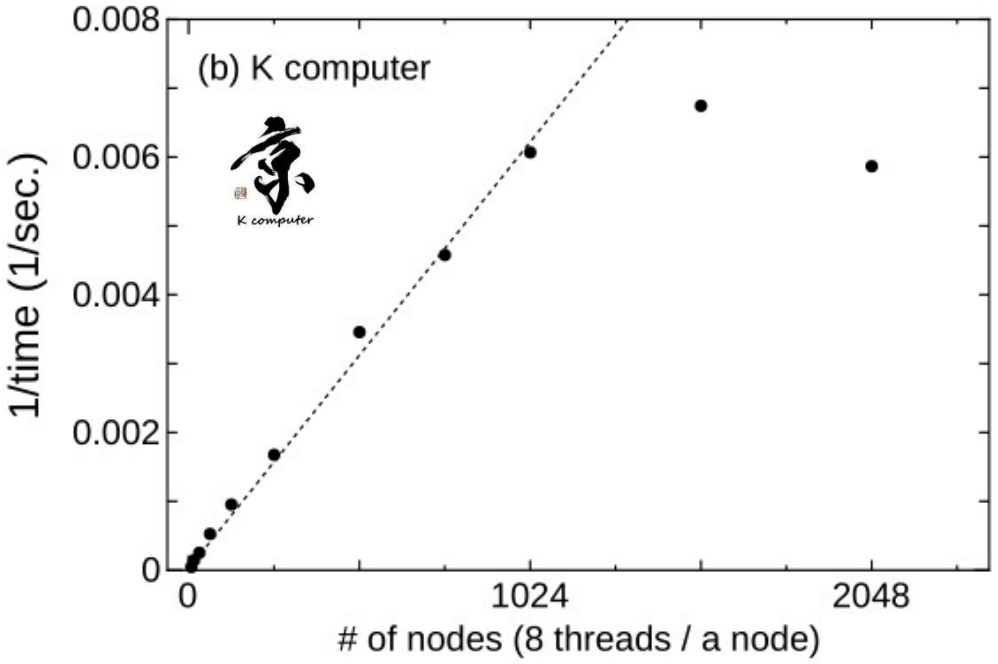

^{56}Ni, pf-shell

10^9 dimension

Good parallel performance up to 10^5 threads

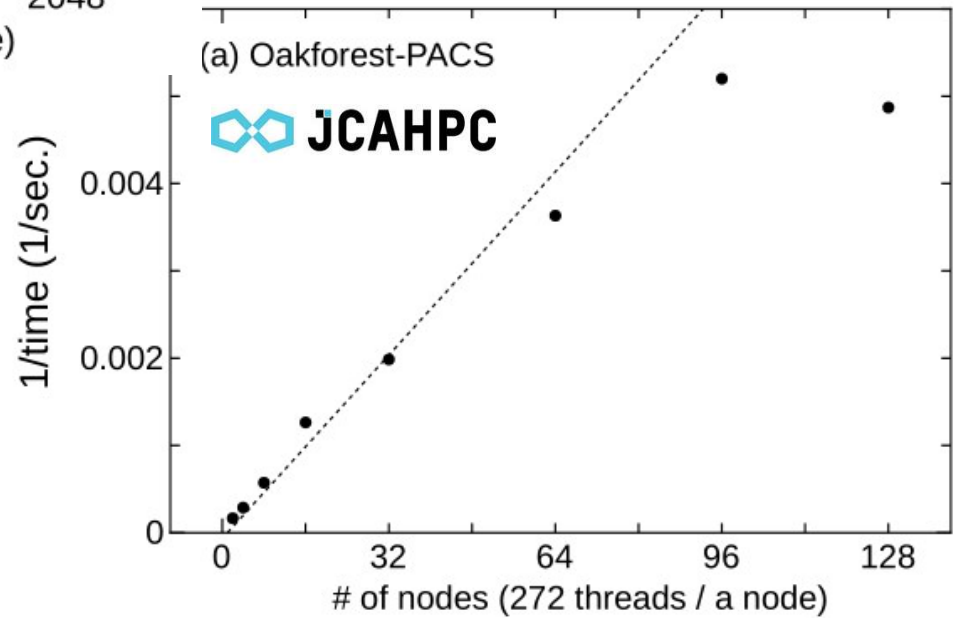

Progress in computer : *M*-scheme dimension vs. year

Computation cost is almost proportional to the *M*-scheme dimension

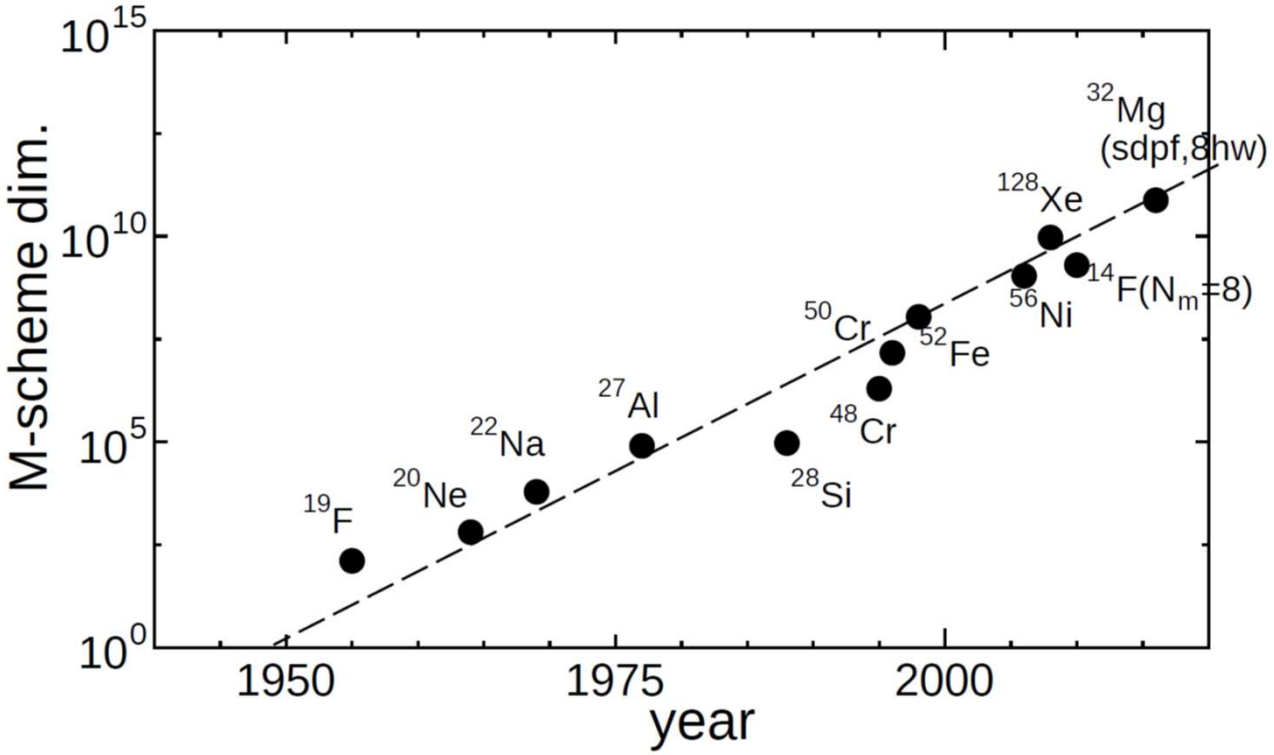

1950 Mayer & Jensen, single-particle SM

Current limit : ~10^{11} M-scheme dim.

⇒ 800 GB / a vector

Odd-mass medium-heavy nuclei

Exp. level scheme of $^{135}_{57}La_{78}$

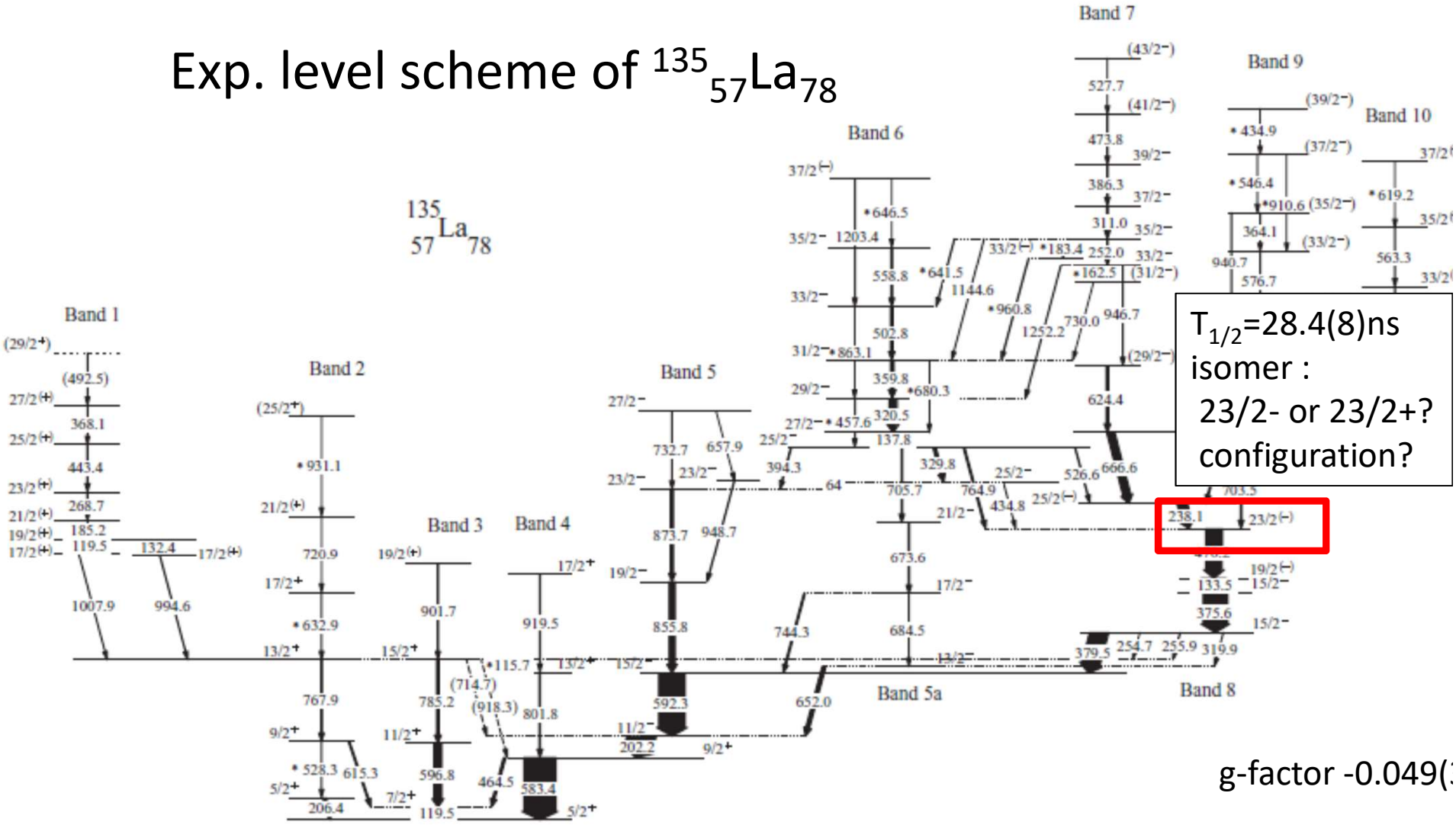

$T_{1/2}$=28.4(8)ns isomer : 23/2- or 23/2+? configuration?

g-factor -0.049(

R. Garg *et al.,* PRC 87, 034317 (2013), R. Leguillion *et al.*, PRC 88, 044309 (2013)

Exp.

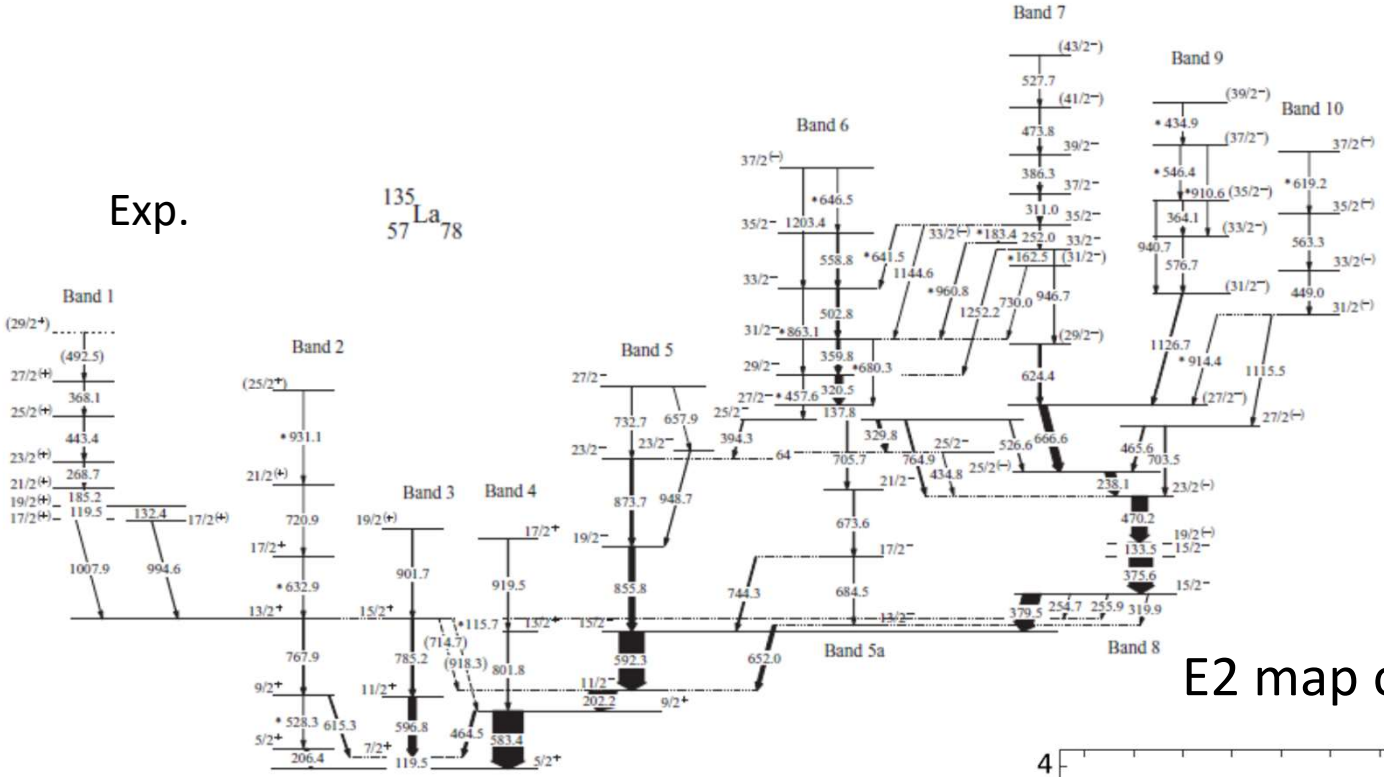

E2 map of 135La

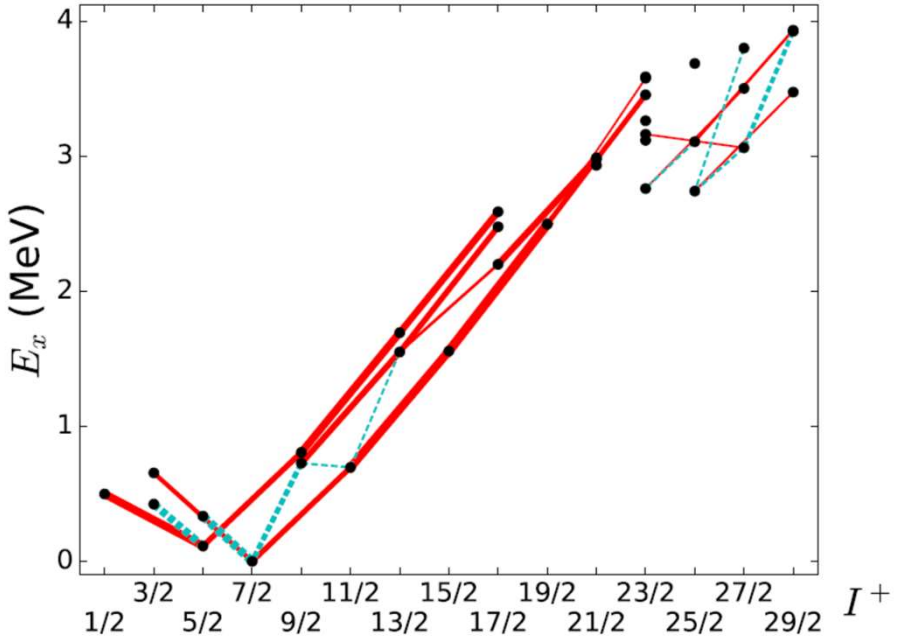

LSSM calculations
50-82 model space,
SNV interaction

$^{135}_{57}La_{78}$: LSSM calc.

Md. S. R. Lasker *et al.* Phys. Rev. C 99 014380 (2019).

Exp.

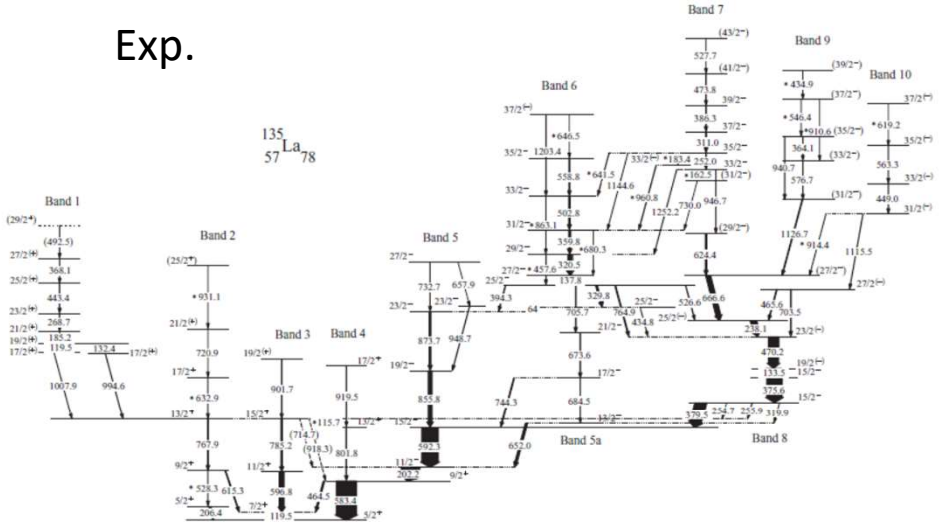

LSSM calc. , arrow width : B(E2)

3 x 10^9 M-scheme dimension

Magnetic rotation

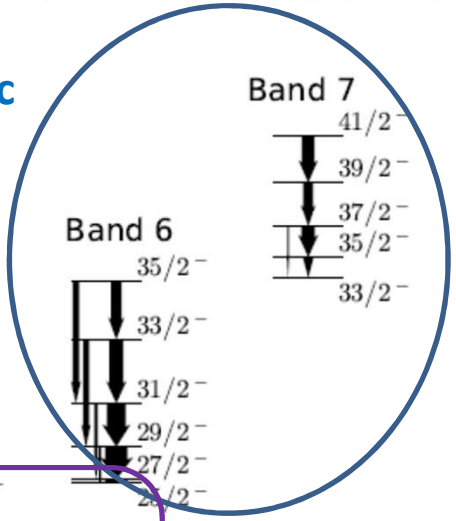

πg7/2 x ^{134}Ba g.b.

πd5/2 x ^{134}Ba g.b.

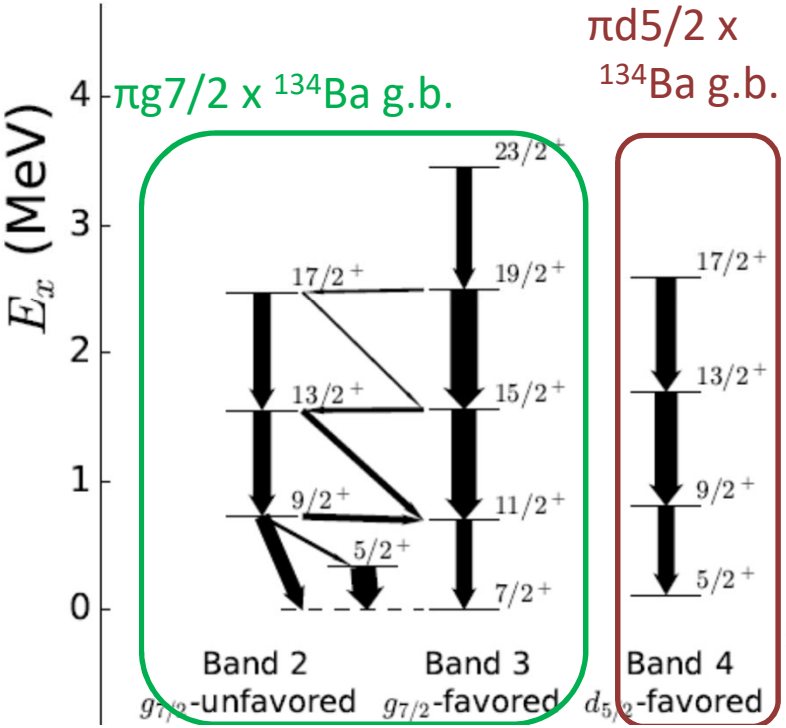

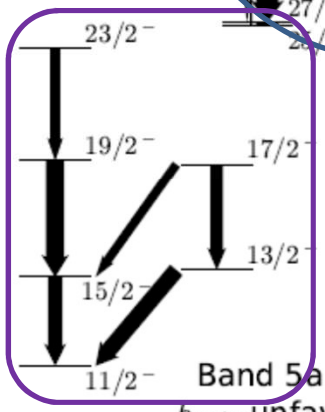

Band 5
$h_{11/2}$-favored

πdh11/2 x ^{134}Ba g.b.

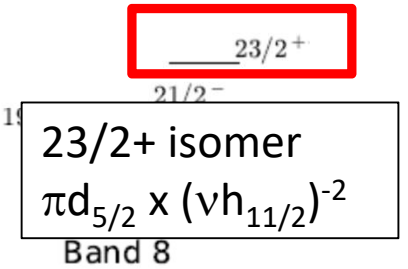

23/2+ isomer

$\pi d_{5/2} \times (\nu h_{11/2})^{-2}$

g-factor -0.049(3)

LSSM -0.052

High-spin states in LSSM: deformed bands of nuclei around ^{40}Ca

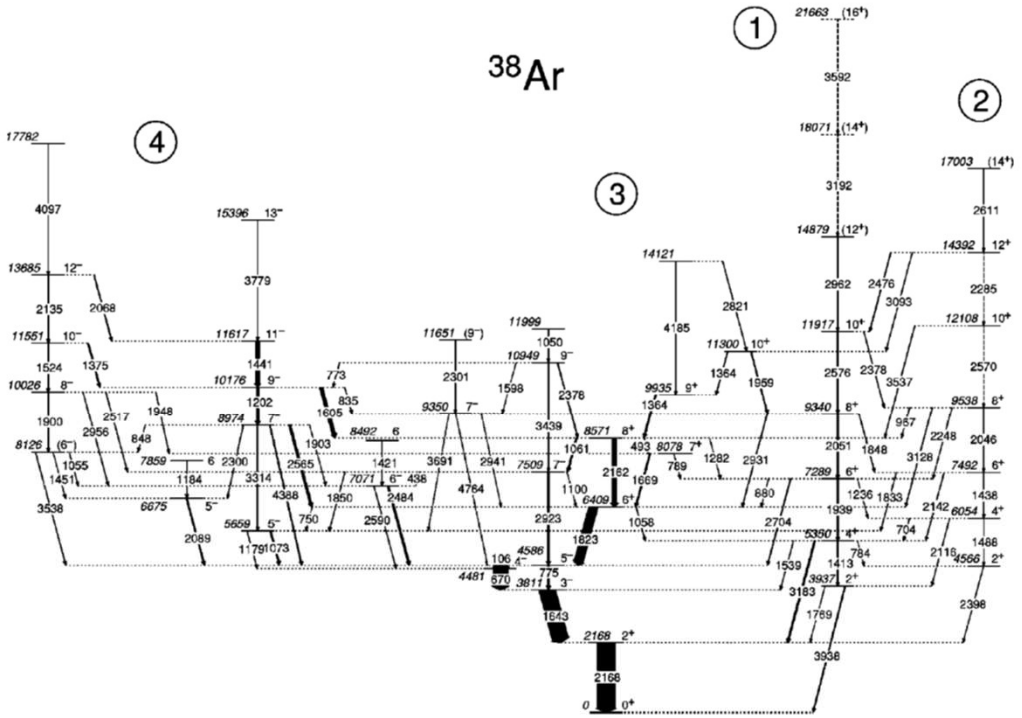

D. Rudolph et al., Phys. Rev. C 65, 034305 (2002)

E2 map of LSSM

sd+f7p3 model space

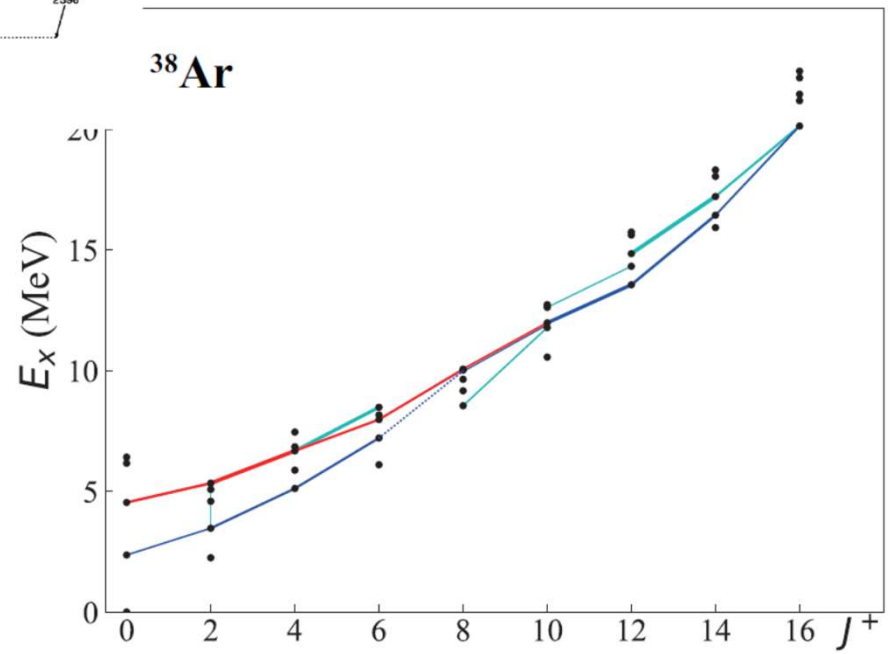

High-spin states in LSSM: deformed bands of nuclei around ^{40}Ca

Y. Utsuno, T. Ichikawa *et al.*

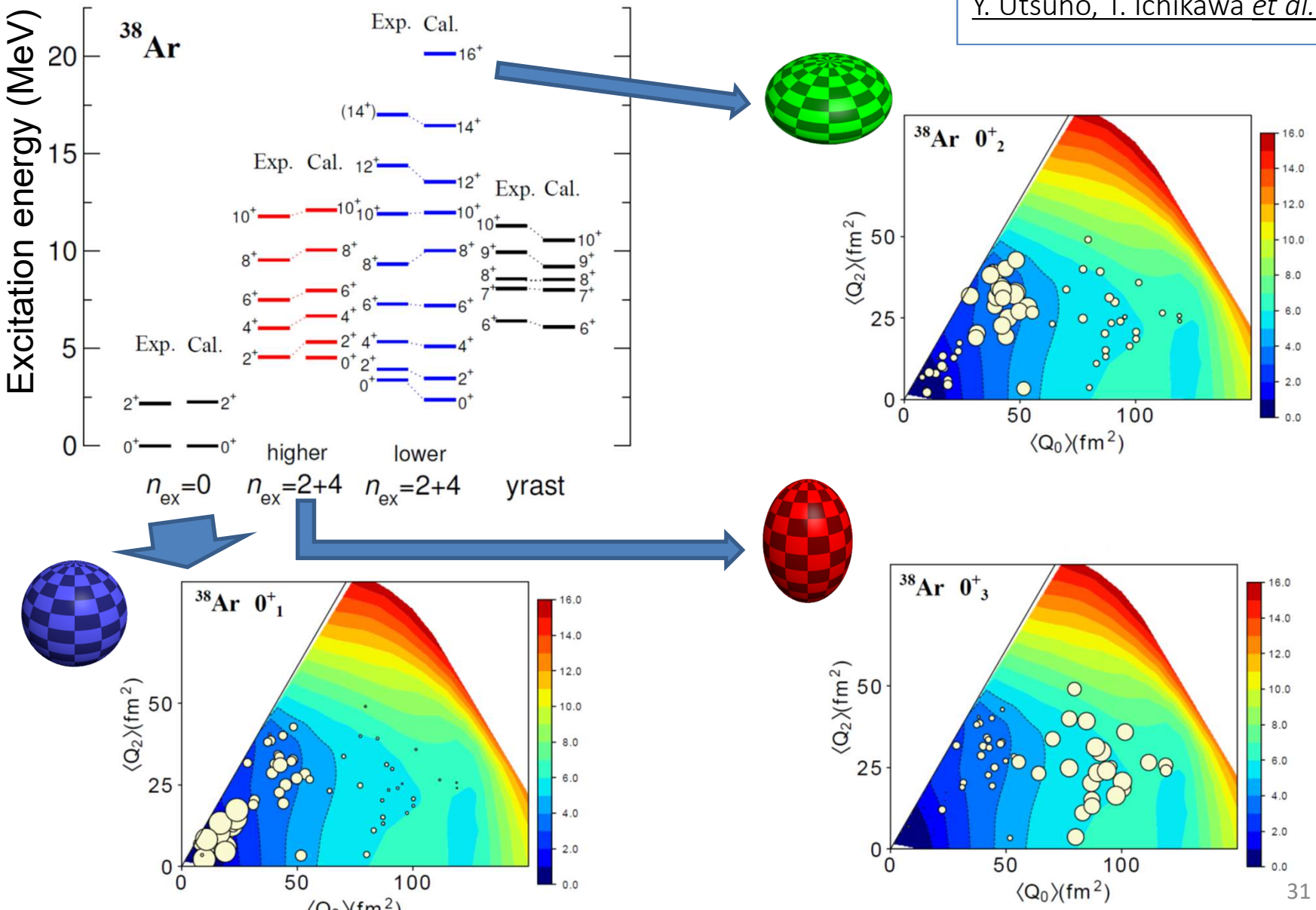

High-spin states in LSSM: deformed bands of nuclei around ^{40}Ca

Y. Utsuno, T. Ichikawa *et al.*

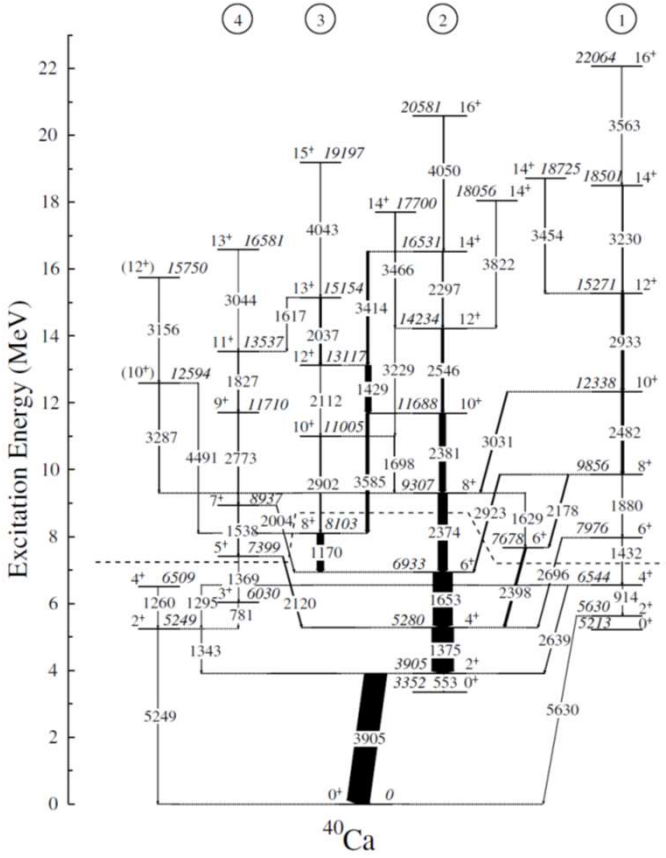

E. Ideguchi et al., Phys. Rev. Lett. 87, 222501 (2001).

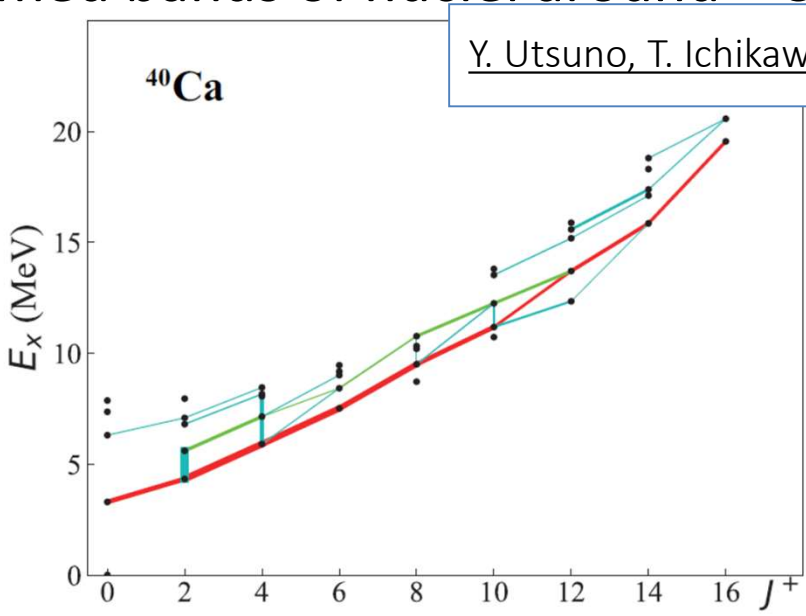

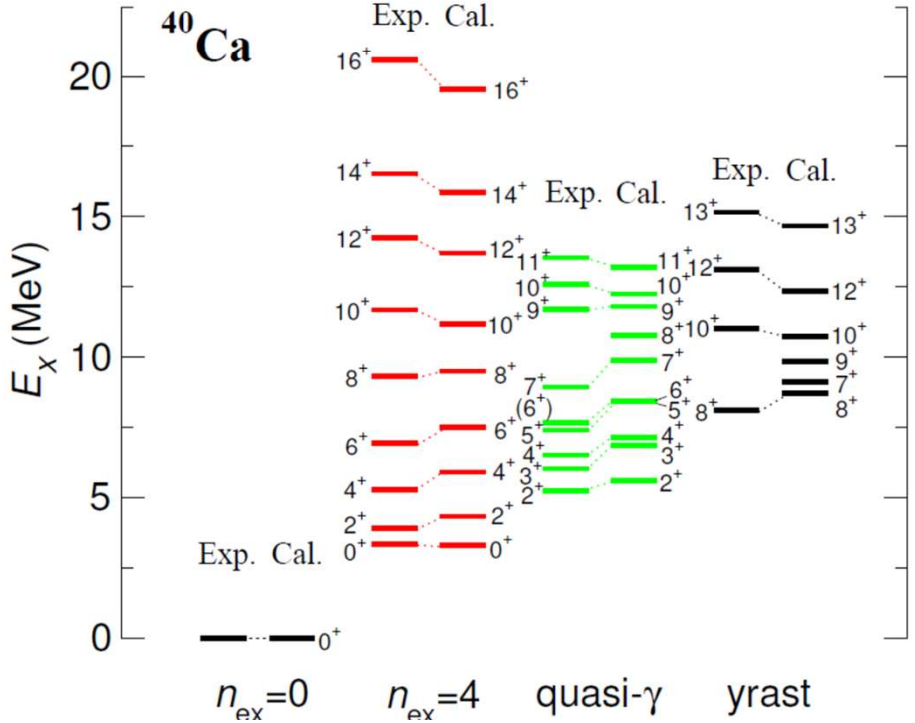

Summary

- Algorithm of the “KSHELL” code: on-the-fly generation of the matrix elements at every matrix-vector product in the Lanczos method.
- Thick-restart block Lanczos method improves the performance.
- Good parallel efficiency for massively parallel computation.
- Feasibility of the LSSM to study high-spin states and deformed bands are demonstrated.

Collaborators

- Takashi Abe (CNS Tokyo)
- Michio Honma (Aizu)
- Takatoshi Ichikawa (CNS Tokyo)
- Takahiro Mizusaki (Senshu)
- Takaharu Otsuka (Tokyo / RIKEN)
- Naofumi Tsunoda (CNS Tokyo)
- Yusuke Tsunoda (CNS Tokyo)
- Yutaka Utsuno (JAEA / CNS Tokyo)
- Sota Yoshida (Tokyo)

and a lot … Thank you!